

# Simulation and Implementation of Three-Input Dc–Dc Boost Converter for Hybrid Pv/Fc/Battery Power System

Senjam Dayananda<sup>1</sup>, Mrs.Naharenjini.N<sup>2</sup>

<sup>1</sup>PG student, Department of Electrical and Electronics Engineering Hindustan University Chennai, India

<sup>2</sup>Assistant professor, Department of Electrical and Electronics Engineering Hindustan University Chennai, India

## Abstract

A new three-input dc–dc boost converter is proposed in this paper. The proposed converter interfaces two unidirectional input power ports and a bidirectional port for a storage element in a unified structure. This converter is interesting for hybridizing alternative energy sources such as photovoltaic (PV) source, fuel cell (FC) source, and battery. Supplying the output load, charging or discharging the battery can be made by the PV and the FC power sources individually or simultaneously. The proposed structure utilizes only four power switches that are independently controlled with four different duty ratios. Utilizing these duty ratios, tracking the maximum power of the PV source, setting the FC power, controlling the battery power, and regulating the output voltage are provided. Depending on utilization state of the battery, three different power operation modes are defined for the converter. In order to design the converter control system, small-signal model is obtained in each operation mode. Due to interactions of converter control loops, decoupling network is used to design separate closed-loop controllers. The validity of the proposed converter and its control performance are verified by simulation and experimental results for different operation conditions.

**Index Terms**—Decoupling method, photovoltaic/fuel cell (PV/FC)/battery hybrid power system, small-signal modeling, state-space averaging, three-input dc–dc boost converter.

## 1.Introduction

Nowadays, photovoltaic (PV) energy appears quite attractive for electricity generation because of its noiseless, pollution-free, scale flexibility, and little maintenance. Because of the PV power generation dependence on sun irradiation level, ambient temperature, and unpredictable shadows, a PV-based power system should be supplemented by other alternative energy sources to ensure a reliable power supply. Fuel cells (FCs) are emerging as a promising supplementary power sources due to their merits of cleanness, high efficiency, and high reliability. Because of long start-up period and slow dynamic response weak points of FCs [1], mismatch power between the load and the FC must be managed by an energy storage system. Batteries are usually taken as storage mechanisms for smoothing output power, improving start-up transitions and dynamic characteristics, and enhancing the peak power capacity [2], [3]. Combining such energy sources

introduces a PV/FC/battery hybrid power system. In comparison with single-sourced systems, the hybrid power systems have the potential to provide high quality, more reliable, and efficient power. In these systems with a storage element, the bidirectional power flow capability is a key feature at the storage port. Further, the input power sources should have the ability of supplying the load individually and simultaneously. Many hybrid power systems with various power electronic converters have been proposed in the literature up to now. Traditional methods that integrate different power sources to form a hybrid power system can be classified into ac-coupled systems and ac-coupled systems [4], [5] and ac-coupled systems [6],[7]. However, the main shortcomings of these traditional integrating methods are complex system topology, high count of devices, high power losses, expensive cost, and large size. In recent years, several power conversion stages used in traditional hybrid systems are replaced by multi-input converters (MICs), which combine different power sources in a single power structure. These converters have received more attention in the literature because of providing simple circuit topology, centralized control, bidirectional power flow for the storage element, high reliability, and low manufacturing cost and size. In general, the systematic approach of generating MICs, in which the concept of the pulsating voltage source cells and the pulsating current source cells is proposed for deriving MICs. There are two types of MICs: in the first type, only one power source is allowed to transfer energy to the load at a time, and in the second type, all the input sources can deliver power to the load either individually or simultaneously. As another basic research in MICs, assumptions, restrictions, and conditions used in analyzing MICs are described, and then it lists some basic rules that allow determining feasible and unfeasible input cells that realize MICs from their single-input versions.

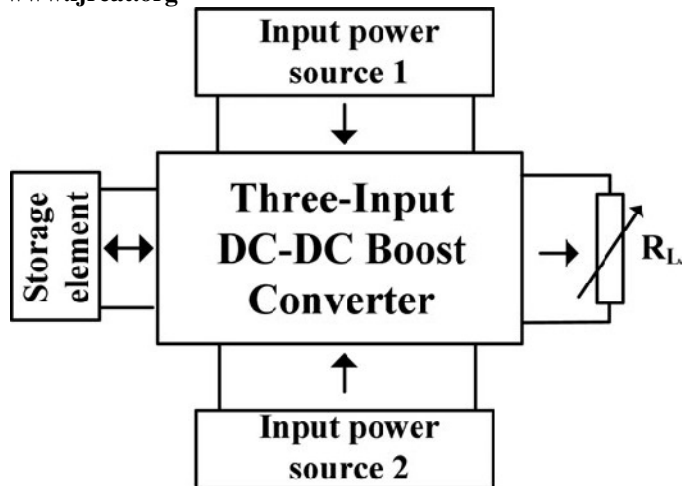


Fig.1. Proposed system overview

In this paper, a new three-input dc–dc boost converter is proposed for hybrid power system applications. As shown in Fig. 1, the proposed converter interfaces two unidirectional ports for input power sources, a bidirectional port for a storage element, and a port for output load in a unified structure. The converter is current-source type at the both input power ports and is able to step up the input voltages. The proposed structure utilizes only four power switches that are independently controlled with four different duty ratios. Utilizing these duty ratios facilitates controlling the power flow among the input sources and the load. Powers from the input power sources can be delivered to the load individually or simultaneously. Moreover, the converter topology enables the storage element to be charged or discharged through both input power sources. Depending on utilization state of the storage element; three different power operation modes of the converter are defined.

As an interesting application of the proposed converter, the input ports are mainly considered to interface a PV source and an FC source, and a battery as the storage element. In this application, achieving the maximum power of the PV source, setting power of the FC, charging or discharging the battery, and also regulating the output voltage are realized by utilizing the converter duty ratios.

#### Converter structure and operation modes

The structure of the proposed three-input dc–dc boost converter is represented in Fig. 2. As seen from the figure, the converter interfaces two input power sources  $v_1$  and  $v_2$ , and a battery as the storage element. The proposed converter is suitable alternative for hybrid power systems of PV, FC, and wind sources. Therefore,  $v_1$  and  $v_2$  are shown as two dependent power sources that their output characteristics are

determined by the type of input power sources. For example, for a PV source at the first port,  $v_1$  is identified as a function of its current  $i_{L1}$ , light intensity, and ambient temperature. In the converter structure, two inductors  $L_1$  and  $L_2$  make the input power ports as two current type sources, which result in drawing smooth dc currents from the input power sources. The  $RL$  is the load resistance, which can represent the equivalent power feeding an inverter. Four power switches  $S_1$ ,  $S_2$ ,  $S_3$ , and  $S_4$  in the converter structure are the main controllable elements that control the power flow of the hybrid power system.

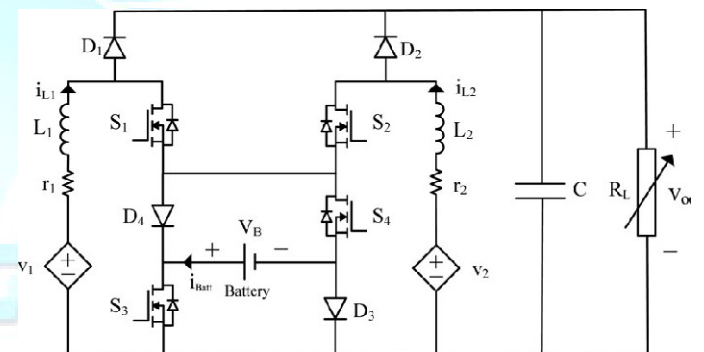


Fig. 2. Circuit topology of the proposed system.

The circuit topology enables the switches to be independently controlled through four independent duty ratios  $d_1$ ,  $d_2$ ,  $d_3$ , and  $d_4$ , respectively. As like as the conventional boost converters, diodes  $D_1$  and  $D_2$  conduct in complementary manner with switches  $S_1$  and  $S_2$ . The converter structure shows that when switches  $S_3$  and  $S_4$  are turned ON, their corresponding diodes  $D_3$  and  $D_4$  are reversely biased by the battery voltage and then blocked. On the other hand, turn-OFF state of these switches makes diodes  $D_3$  and  $D_4$  able to conduct input currents  $i_{L1}$  and  $i_{L2}$ . In hybrid power system applications, the input power sources should be exploited in continuous current mode (CCM). For example, in the PV or FC systems, an important goal is to reach an acceptable current ripple in order to set their output power on desired value. Therefore, the current ripple of the input sources should be minimized to make an exact power balance among the input powers and the load. Therefore, in this paper, steady state and dynamic behaviour of the converter have been investigated in CCM.

In general, depending on utilization state of the battery, three power operation modes are defined to the proposed converter. These modes of operation are investigated with the assumptions of utilizing the same sawtooth carrier waveform for all the switches, and  $d_3, d_4 < \min(d_1, d_2)$  in battery charge or discharge mode. Although exceeding duty ratios  $d_3$

and  $d_4$  from  $d_1$  or  $d_2$  does not cause converter malfunction, it results in setting the battery power on the possible maximum values. In order to simplify the investigations, it is assumed that duty ratio  $d_1$  is less than duty ratio  $d_2$ . Further, with the assumption of ideal switches, the steady-state equations are obtained in each operation mode.

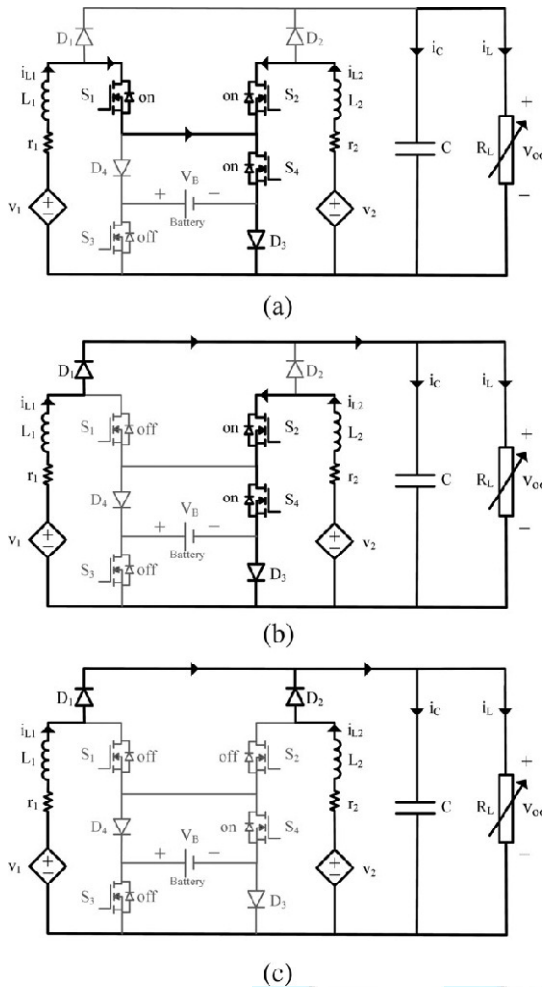


Fig. 3. First operationmode. (a) Switching state 1:  $0 < t < d_1 T$ . (b) Switching state 2:  $d_1 T < t < d_2 T$ . (c) Switching state 3:  $d_2 T < t < T$ .

### A. First Power Operation Mode (Supplying the Load With Sources $v_1$ and $v_2$ Without Battery Existence)

In this operation mode, two input power sources  $v_1$  and  $v_2$  are responsible for supplying the load, and battery charging/discharging is not done. This operation mode is considered as the basic operation mode of the converter. As clearly seen from the converter structure, there are two options

to conduct input power sources currents  $i_{L1}$  and  $i_{L2}$  without passing through the battery; path 1:  $S_4$ – $D_3$ , path 2:  $S_3$ – $D_4$ . In this operation mode, the first path is chosen; therefore, switch  $S_3$  is turned OFF while switch  $S_4$  is turned ON entirely in the switching period ( $d_4 = 1$  and  $d_3 = 0$ ). Thus, three different switching states of the converter are achieved in one switching period. These switching states are depicted in Fig. 3(a)–(c). Also, the steady-state waveforms of the gate signals of the four switches and the variations of inductors currents  $i_{L1}$  and  $i_{L2}$  are shown in Fig. 6(a).

Switching state 1 ( $0 < t < d_1 T$ ): At  $t = 0$ , switches  $S_1$  and  $S_2$  are turned ON and inductors  $L_1$  and  $L_2$  are charged with voltages across  $v_1$  and  $v_2$ , respectively [see Fig. 3(a)].

Switching state 2 ( $d_1 T < t < d_2 T$ ): At  $t = d_1 T$ , switch  $S_1$  is turned OFF, while switch  $S_2$  is still ON (according to the assumption  $d_1 < d_2$ ). Therefore, inductor  $L_1$  is discharged with

voltage across  $v_1 - v_o$  into the output load and the capacitor through diode  $D_1$ , while inductor  $L_2$  is still charged by voltage across  $v_2$  [see Fig. 3(b)].

Switching state 3 ( $d_2 T < t < T$ ): At  $t = d_2 T$ , switch  $S_2$  is also turned OFF and inductor  $L_2$  is discharged with voltage across  $v_2 - v_o$ , as like as inductor  $L_1$  [see Fig. 3(c)]. By applying voltage–second and current–second balance theory to the converter, following equations are obtained:

$$L_1: d_1 T(v_1 - r_1 i_{L1}) + (1 - d_1)T(v_1 - r_1 i_{L1} - v_o) = 0 \rightarrow v_o = \frac{v_1 - r_1 i_{L1}}{1 - d_1} \quad (1)$$

$$L_2: d_2 T(v_2 - r_2 i_{L2}) + (1 - d_2)T(v_2 - r_2 i_{L2} - v_o) = 0 \rightarrow v_o = \frac{v_2 - r_2 i_{L2}}{1 - d_2} \quad (2)$$

$$C: (1 - d_1)T i_{L1} + (1 - d_2)T i_{L2} = T \frac{v_o}{R_L} \quad (3)$$

$$i_{\text{batt}} = 0 \rightarrow P_{\text{batt}} = 0. \quad (4)$$

In this operation mode, the control strategy is based on regulating one of the input sources on its reference power with its corresponding duty ratio, while the other power source is utilized to regulate the output voltage by means of its duty ratio.

### B. Second Power Operation Mode (Supplying the Load With Sources $v_1$ and $v_2$ and the Battery)

In this operation mode, two input power sources  $v_1$  and  $v_2$  along with the battery are responsible for supplying the load. Therefore, discharging state of the battery should be provided in this operation mode. Referring to the converter topology, when switches  $S_3$  and  $S_4$  are turned ON simultaneously, currents  $i_{L1}$  and  $i_{L2}$  are conducted through the path of switch  $S_4$ , the battery, and switch  $S_3$  which results in battery discharging. However, discharging operations of the battery

can only last until switches S1 and/or S2 are conducting. As a result, the maximum discharge power of the battery depends on duty ratios of d1 and d2 as well as currents iL1 and iL2 :

$$P_{bat\ dis}^{max} = v_B [d_1 i_{L1} + d_2 i_{L2}], S_3 = ON, S_4 = ON. \quad (5)$$

Therefore, in order to acquire a desired maximum discharging power of the battery, the input power sources should be designed in proper current and voltage values. On the other hand, regulating the discharging power of the battery below  $P_{bat\ dis}^{max}$  can be made by changing the state of only one of switches S3 and S4 before switches S1 and S2 are turned OFF (according to the assumption  $d_3, d_4 < \min(d_1, d_2)$ ). In this paper, duty ratio d4 is controlled to regulate the discharging power of the battery regarding the facts that when S4 is turned ON, it results in passing the currents of input power sources through the battery; hence, the battery discharge mode is started, and its turn-OFF state starts conducting through diode D4 and stops discharging the battery. As depicted in Fig. 4(a)–(d), there are four different switching states for the converter in one switching period. The steady-state waveforms of the gate signals of the four switches and the variations of input currents iL1 and iL2 are shown in Fig. 6(b).

Switching state 1 ( $0 < t < d_4 T$ ): At  $t = 0$ , switches S1, S2, and S4 are turned ON, so inductors L1 and L2 are charged with voltages across  $v_1 + v_B$  and  $v_2 + v_B$ , respectively [see Fig. 4(a)].

Switching state 2 ( $d_4 T < t < d_1 T$ ): At  $t = d_4 T$ , switch S4 is turned OFF, while switches S1 and S2 are still ON. Therefore, inductors L1 and L2 are charged with voltages across  $v_1$  and  $v_2$  respectively [see Fig. 4(b)].

Switching state 3 ( $d_1 T < t < d_2 T$ ): At  $t = d_1 T$ , switch S1 is turned OFF, so inductor L1 is discharged with voltage across  $v_1 - v_o$ , while inductor L2 is still charged with voltages across  $v_2$  [see Fig. 4(c)].

Switching state 4 ( $d_2 T < t < T$ ): At  $t = d_2 T$ , switch S2 is also turned OFF and inductors L1 and L2 are discharged with voltage across  $v_1 - v_o$  and  $v_2 - v_o$ , respectively [see Fig. 4(d)].

By applying voltage–second and current–second balance theory to the converter, following equations are obtained:

$$L_1: d_4 T(v_1 - r_1 i_{L1} + v_B) + (d_1 - d_4) T(v_1 - r_1 i_{L1}) + (1 - d_1) T(v_1 - r_1 i_{L1} - v_o) = 0$$

$$\rightarrow v_o = \frac{v_1 - r_1 i_{L1} + d_4 v_B}{1 - d_1} \quad (6)$$

$$L_2: d_4 T(v_2 - r_2 i_{L2} + v_B) + (d_2 - d_4) T(v_2 - r_2 i_{L2})$$

$$+ (1 - d_2) T(v_2 - r_2 i_{L2} - v_o) = 0$$

$$\rightarrow v_o = \frac{v_2 - r_2 i_{L2} + d_4 v_B}{1 - d_2} \quad (7)$$

$$C: (1 - d_1) T i_{L1} + (1 - d_2) T i_{L2} = T \frac{v_o}{R_L} \quad (8)$$

$$\text{Battery} \begin{cases} i_{Batt} = d_4 (i_{L1} + i_{L2}) \\ P_{Batt} = v_B [d_4 (i_{L1} + i_{L2})]. \end{cases} \quad (9)$$

In this operation mode, the control strategy is based on regulating both of the input power sources on their reference powers by means of their corresponding duty ratios d1 and d2, while the battery discharge power is utilized to regulate the output voltage by duty ratio d4.

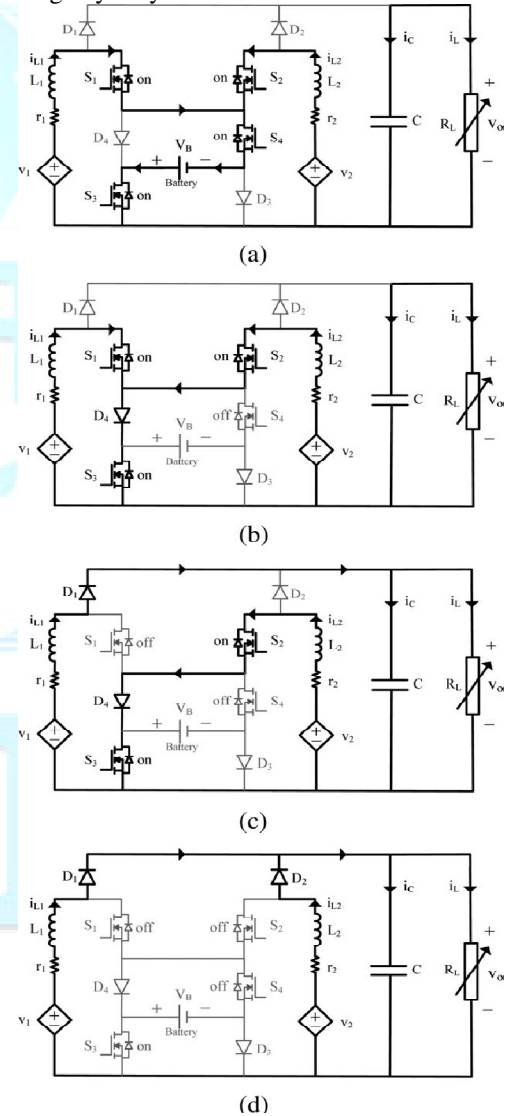


Fig. 4. Second operation mode. (a) Switching state 1:  $0 < t < d_4 T$ . (b) Switching state 2:  $d_4 T < t < d_1 T$ . (c) Switching state 3:  $d_1 T < t < d_2 T$ . (d) Switching state 4:  $d_2 T < t < T$ .

C. Third Power Operation Mode (Supplying the Load With Sources v1 and v2 , and Battery Charging Performance)

In this operation mode, two input power sources v1 and v2 are responsible for supplying the load while the battery charging performance is accomplished. Therefore, the charging state of the battery should be provided in this operation mode. Referring to the converter topology, when switches S3 and S4 are turned OFF, by turning ON switches S1 and S2 , currents iL 1 and iL 2 are conducted through the path of diode D4 , the battery, and diode D3 ; therefore, the condition of battery charging is provided. However, the charging operation of the battery can only last until switches S1 and/or S2 are conducting. As a result, the maximum charge power of the battery depends on duty ratios d1 and d2 as well as currents iL 1 and iL 2 :

$$P_{bat\ dis}^{max} = -v_B [d_1 i_{L1} + d_2 i_{L2}], S_3 = OFF, S_4 = OFF. \quad (10)$$

Therefore, in order to acquire a desired maximum charge power of the battery, the input power sources should be designed in proper current and voltage values. On the other hand, regulating the charging power of the battery below the  $P_{bat\ dis}^{max}$  can be made by changing the state of only one of switches S3 and S4 before switches S1 and S2 are turned OFF (according to the assumption  $d_3, d_4 < \min(d_1, d_2)$  ). In this paper, in order to regulate the charging power of the battery, switch S3 is controlled by regarding the fact that when switch S3 is turned ON, the charging power of the battery is not accomplished while its turn-OFF state make the battery to be charged with currents iL1 and iL 2 through the path of D3 . Four different switching state occurred in one switching period are illustrated in Fig. 5(a)–(d). Also, the steady-state waveforms of the gate signals of the four switches and the variations of input currents iL 1 and iL 2 are shown in the Fig. 6(c).

Switching state 1 ( $0 < t < d_3 T$ ): At  $t = 0$ , switches S1 , S2 , and S3 are turned ON, so inductors L1 and L2 are charged with voltages across v1 and v2 , respectively [see Fig. 5(a)].

Switching state 2 ( $d_3 T < t < d_1 T$ ): At  $t = d_3 T$ , switch S3 is turned OFF while switches S1 and S2 are still ON (according to the assumption). Therefore, inductors L1 and L2 are charged with voltages across  $v1 - v_B$  and  $v2 - v_B$  , respectively [see Fig. 5(b)].

Switching state 3 ( $d_1 T < t < d_2 T$ ): At  $t = d_1 T$ , switch S1 is turned OFF, so inductor L1 is discharged with voltage across  $v1 - v_o$  , while inductor L2 is still charged with voltage across  $v2 - v_B$  [see Fig. 5(c)].

Switching state 4 ( $d_2 T < t < T$ ): At  $t = d_2 T$ , switch S2 is also turned OFF and inductor L2 as like as L1 is discharged with voltage across  $v2 - v_o$  [see Fig. 5(d)].

By applying voltage–second and current–second balance theory to the converter, following equations are obtained:

$$L_1: d_3 T(v_1 - r_1 i_{L1}) + (d_1 - d_3)T(v_1 - r_1 i_{L1} - v_B) + (1 - d_1)T(v_1 - r_1 i_{L1} - v_o) = 0$$

$$\rightarrow v_o = \frac{v_1 - r_1 i_{L1} - (d_1 - d_3)v_B}{1 - d_1} \quad (11)$$

$$L_2: d_2 T(v_2 - r_2 i_{L2}) + (d_2 - d_3)T(v_2 - r_2 i_{L2} - v_B) + (1 - d_2)T(v_2 - r_2 i_{L2} - v_o) = 0$$

$$\rightarrow v_o = \frac{v_2 - r_2 i_{L2} - (d_2 - d_3)v_B}{1 - d_2} \quad (12)$$

$$C: (1 - d_1)T i_{L1} + (1 - d_2)T i_{L2} = T \frac{v_o}{R_L} \quad (13)$$

$$\text{Battery} \begin{cases} i_{Batt} = (d_1 - d_3)i_{L1} - (d_2 - d_3)i_{L2} \\ P_{Batt} = -v_B [(-d_3)(i_{L1} + i_{L2}) + d_1 i_{L1} + d_2 i_{L2}]. \end{cases} \quad (14)$$

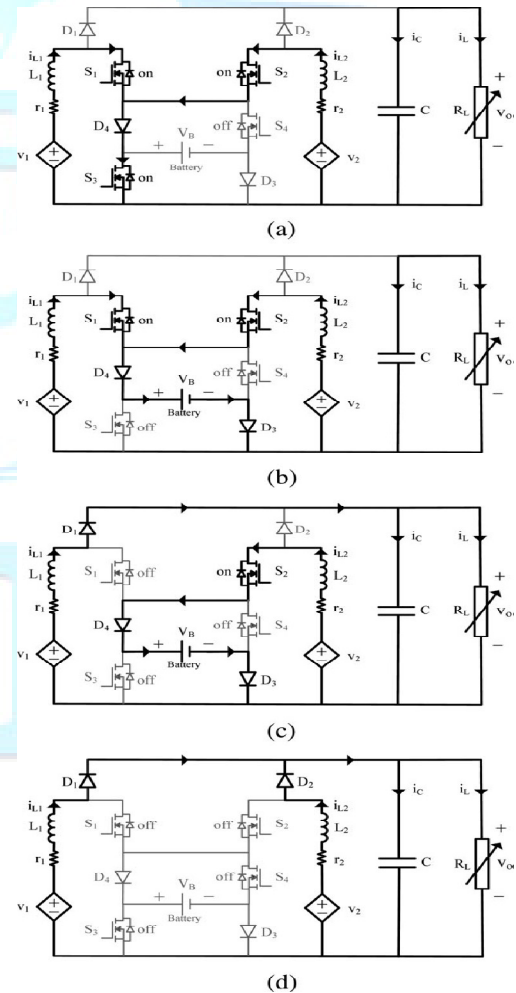


Fig. 5. Third operationmode. (a) Switching state 1:  $0 < t < d_3 T$ . (b) Switching state 2:  $d_3 T < t < d_1 T$ . (c) Switching state 3:  $d_1 T < t < d_2 T$ . (d) Switching state 4:  $d_2 T < t < T$ .

In this operation mode, if the total generated power of the input sources becomes more than the load power, the battery charging performance will be possible if duty ratio  $d_3$  is utilized to regulate the output voltage. With this control strategy, duty ratios  $d_1$  and  $d_2$  are utilized to regulate powers of the input sources, while duty ratio  $d_3$  is utilized to regulate the output voltage through charging the battery by the extra-generated power.

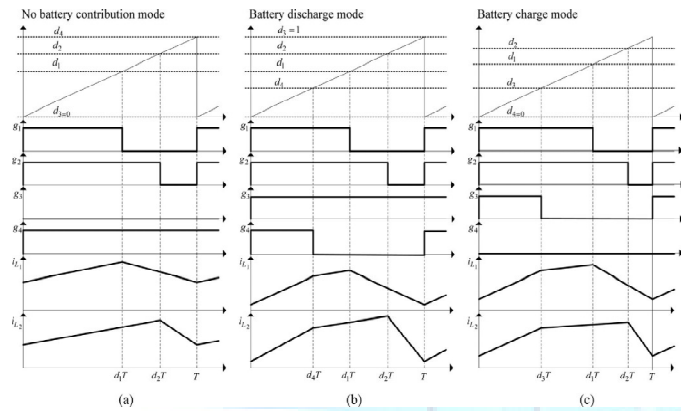


Fig. 6. Steady-state waveform of proposed converter in (a) first operation mode, (b) second operation mode, and (c) third operation mode.

In all three operation modes, when one of the input power sources is not present to produce power, its corresponding duty ratio is set at zero, which results single power source operation for the converter.

### 3.SIMULATION AND RESULT

Matlab Circuit Diagram:

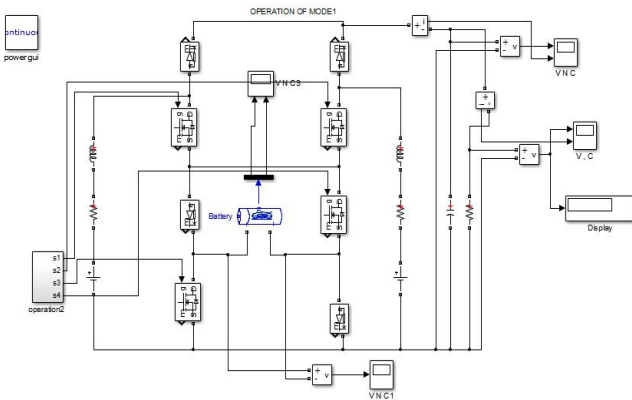


Fig. 7 Simulation Circuit.

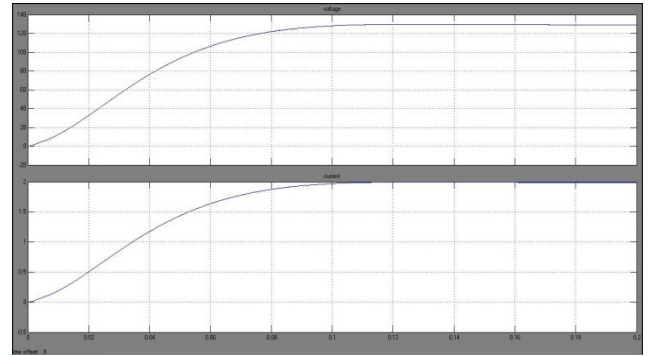


Fig. 8 Mode 1 Voltage and Current Output.

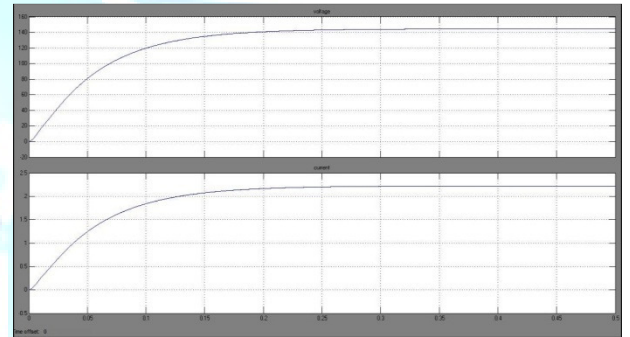


Fig. 9 Mode 2 Voltage and Current Output.

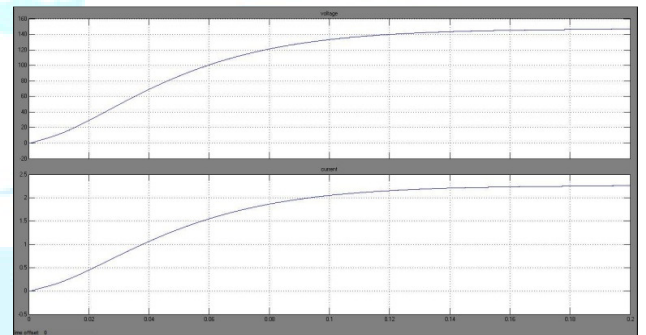


Fig. 10 Mode 3 Voltage and Current Output.

In the simulations, achieving the maximum power of the PV source, setting power of the FC, charging or discharging the battery, and also regulating the output voltage are realized by utilizing the converter duty ratios.

### 4. CONCLUSION

The control of a three input DC-DC boost converter for hybrid PV/FC/Battery power system is obtained. The Simulink model has been simulated in MATLAB. The resulting voltage and current graphs of each of the three modes has been studied.

## REFERENCES

- [1] W. Jiang and B. Fahimi, "Active current sharing and source management in fuel cell-battery hybrid power system," IEEE Trans. Ind. Electron., vol. 57, no. 2, pp. 752–761, Feb. 2010.
- [2] R. J. Wai, Ch. Y. Lin, J. J. Liaw, and Y. R. Chang, "Newly designed ZVS multi-input converter," IEEE Trans. Ind. Electron., vol. 58, no. 2, pp. 555–566, Feb. 2011.
- [3] J. L. Duarte, M. Hendrix, and M. G. Simoes, "Three-port bidirectional converter for hybrid fuel cell systems," IEEE Trans. Power Electron., vol. 22, no. 2, pp. 480–487, Mar. 2007.
- [4] N. Kato, K. Kurozumi, N. Susuld, and S. Muroyama, "Hybrid power-Supply system composed of photovoltaic and fuel-cell systems," in Proc Int. Telecommun. Energy Conf., 2001, pp. 631–635.
- [5] K. Rajashekara, "Hybrid fuel-cell strategies for clean power generation," IEEE Trans. Ind. Appl., vol. 41, no. 3, pp. 682–689, May/Jun.2005.
- [6] P. Thounthong, S. Rael, and B. Davat, "Control strategy of fuel cell and supercapacitor association for a distributed generation system," IEEE Trans. Ind. Electron., vol. 56, no. 6, pp. 3225–3233, Dec.2007.
- [7] O. C. Onara, M. Uzunoglu, and M. S. Alam, "Modeling, control and simulation of an autonomous wind turbine/photovoltaic/fuel cell/ultra capacitor hybrid power system," *J. Power Sources.*, vol. 185, no. 2, pp 1273–1283, Apr. 2008.

PRDGG